Available online at www.sciencedirect.com

SciVerse ScienceDirect

journal homepage: www.elsevier.com/locate/he

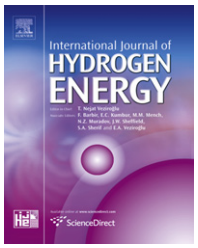

Alloying and surface composition of model Pd–Ag films synthesized by electroless deposition

*A.M. Tarditi, M.L. Bosko, L.M. Cornaglia**

Instituto de Investigaciones en Catálisis y Petroquímica (FIQ, UNL-CONICET), Santiago del Estero 2829, 3000 Santa Fe, Argentina

ARTICLE INFO

Article history:
Received 28 October 2011
Received in revised form
1 December 2011
Accepted 21 December 2011
Available online 26 January 2012

Keywords:
PdAg composite membranes
Model samples
Surface segregation
Electroless deposition

ABSTRACT

PdAg model films and real composite membranes were prepared by sequential electroless deposition on top of porous stainless steel supports. Their surface properties were investigated by X-ray photoelectron spectroscopy (XPS), Angle resolved XPS and sputtering depth profile. It was shown that the surface of the alloy was strongly enriched in silver after the annealing treatment up to 500 °C on hydrogen stream. A relationship between the Ag $3d_{5/2}$ core-level binding energy shift and the silver surface composition was observed from the XPS data obtained with the model samples. The surface composition of real membranes after both hydrogen permeation and reaction experiments showed silver enrichment, in agreement with the data obtained from the model sample.

1. Introduction

Surface composition is an important parameter in understanding the behavior of alloys in a wide range of applications such as catalysis and corrosion, and it is often different from bulk composition. The exposure of an alloy to different atmospheres and temperatures can produce preferential surface segregation in either beneficial or detrimental ways. For this reason, a quantitative description of the phenomenon is necessary in order to make the appropriate changes in the bulk alloy composition to enhance or inhibit specific segregation behavior.

Regarding surface segregation effects on PdAg alloys, several theoretical and experimental studies have been reported even though they reveal some degree of discrepancy [1,2]. The surface enrichment of silver was reported in the case of PdAg alloys in a vacuum or inert atmosphere in agreement with the lower surface energy of silver [2]. This situation could change when adsorbates are in contact with the alloy surface leading to adsorbate-induced segregation or disegregation of binary metal alloys [2]. Interestingly, a reverse surface segregation of palladium in a PdAg membrane after exposure to H_2 was reported by Opalka and co-workers [3].

As it is well known, the component distribution on a membrane surface and in the bulk influences the membrane's hydrogen permeation properties. Hence, a deeper understanding of the relationship between the surface states, including structure and composition of the membrane, and its hydrogen permeability may lead to the discovery of new materials with improved hydrogen permeation properties. Sakamoto and co-workers [4,5] examined the effect of methane, ethylene and carbon monoxide on the hydrogen permeation of several Pd-based alloy membranes after permeation experiments. The XPS analysis showed that the intensity of the carbon spectrum decreased with an increase of Ar^+ sputtering. They claimed that the decrease in hydrogen permeability under the mixture gases could be related to the adsorption of the impurity gases on the alloy

* *Corresponding author*. Tel./fax: +54 342 4536861.
E-mail address: lmcornag@fiq.unl.edu.ar (L.M. Cornaglia).

0360-3199/$ – see front matter
doi:10.1016/j.ijhydene.2011.12.128

surfaces, and may be caused by the decrease in effective area for the dissociation of hydrogen molecules. Citing XPS results, Shu et al. [6] reported that hydrogen chemisorption on palladium sites drives strong palladium segregation on the PdAg membrane surface. Bredesen and co-workers [7] used XPS and AES to study the surface segregation effects on PdAg composite membranes after operation. The Ag/Pd ratio increased about 32% after testing at high temperature as evidenced by both XPS and AES data. Recently, Bosko et al. [8] reported the effect of different annealing temperatures in the surface segregation of PdAg membranes synthesized by sequential electroless plating. The XPS data gave an indication of Ag segregation to the Pd–Ag film surfaces under all the conditions studied.

Several methods have been reported in the literature for the deposition of Pd and Pd-alloys on porous substrates such as chemical vapor deposition, sputtering, electroless deposition or e-beam evaporation. Electroless plating has several advantages over the other methods since it is simple, less expensive and allows the formation of uniform layers on several geometries. For this reason, this method has been used by several groups for the fabrication of Pd-based alloy membranes [9–12]. In our group, we adopted consecutive electroless depositions of Pd and Ag to obtain several PdAg-alloy composite membranes [8,13]. In order to form a homogeneous alloy at relative moderate temperatures (~500 °C) without affecting the performance of the membrane, the plating times, temperatures and concentrations were optimized. As previously reported, the use of short deposition times improves the formation of an alloy with homogeneous composition at temperatures as low as 500 °C [13].

The aim of this work was to study the surface segregation behavior of PdAg alloys synthesized by electroless deposition technique. For this purpose, we studied the behavior of two PdAg model samples prepared by this method on top of porous stainless steel disks. Surface and bulk alloy formation and chemical atomic composition of these samples were confirmed prior to surface characterization. In addition, XPS depth profile experiments of PdAg composite tubular membranes were carried out to analyze the surface segregation of these real samples after being exposed to the dry reforming of methane.

2. Experimental

2.1. Sample synthesis

2.1.1. PdAg model samples

In order to study the surface properties of the PdAg binary alloy synthesized by electroless deposition, two samples with a theoretical composition of 10 and 25% of silver (PdAg10 and PdAg25, respectively) were prepared on top of porous stainless steel disks (0.2 μm grade, 12.7 mm in diameter and thickness of 2 mm), provided by Mott Metallurgical Corporation. The supports were cleaned in an alkaline solution and oxidized in stagnant air at 500 °C for 12 h [14]. After that, the supports were modified by dip coating of Al_2O_3, following the procedure previously described in Ref. [8]. The modified disks were activated by the conventional two-step $SnCl_2/PdCl_2$ method [15]. After the activation, the metallic electroless plating was carried out by the sequential deposition of Pd and Ag. Two different deposition times were used during the plating in order to obtain different palladium and silver compositions. After the metal deposition, all samples were annealed at 500 °C in order to promote metallic inter-diffusion and alloy formation. The samples were mounted in a quartz reactor and then they were heated up from room temperature up to 500 °C with a heating rate of 0.5 °C min^{-1} in nitrogen flow. Then, to perform the annealing process, the samples were kept at this temperature in flowing hydrogen during 120 h. This procedure allowed us to obtain a homogeneous alloy composition in thickness.

2.1.2. PdAg composite membranes

Composite PdAg tubular membranes were prepared by sequential electroless plating on the outer surface of porous stainless steel (PSS) tubes purchased from Mott Metallurgical Corporation (0.2 μm grade, 6.4 mm i.d., 9.5 mm o.d.). After cleaning and oxidation, the substrates were modified by either dip coating of Al_2O_3 [8] or in-situ hydrothermal synthesis of ZNaA [16]. The metallic depositions were carried out using the same bath composition and temperature reported elsewhere [16]. In order to obtain a homogeneous alloy composition, a 40-min deposition time was used. Further details regarding metallic deposition were given in previous publications [8,16]. The activation-plating cycle was repeated until the composite PdAg membrane became impermeable to N_2 at room temperature and at a pressure different from 10 kPa. The membranes were heated at 500 °C for 110 h or at 550 °C during 24 h in H_2 atmosphere. During annealing, a pressure difference of 10 kPa was applied. The thickness of the membranes was estimated from the weight gain after palladium-silver deposition and checked by SEM. The nomenclature adopted for the membranes was PdAg-*X*-*Y*/*M*, where *X* refers to plating time, *Y* to annealing temperature and *M* to the substrate modifier.

2.2. Gas permeation measurements

Thermal treatments and gas permeation measurements were conducted in a shell-and-tube membrane module. The open end of the membrane was sealed to the permeator wall with Teflon ferrules. The permeator was placed in an electrical furnace and heated to the desired temperatures. A thermocouple within the membrane tube monitored and controlled the temperature during the experiments. All the gases were fed to the permeator using calibrated mass-flow controllers. Feed gases flowed along the outside of the membrane while the permeated gases flow rates were measured in the inner side of the membrane. A N_2 sweep gas stream was fed in the permeate side only during the heating and cooling periods. Pressure differences across the membranes were controlled using a back-pressure regulator. The upstream was varied while keeping the downstream pressure constant at 100 kPa. The gas permeation flow rates of either H_2 or N_2 were measured using two bubble flow meters at room temperature and pressure. The lowest flux that could be detected by our bubble flow meter was ca. 4×10^{-5} mol m^{-2} s^{-1}.

2.3. Sample characterization

2.3.1. Surface characterization

XPS analyses were performed in a multi-technique system (SPECS) equipped with a dual Mg/Al X-ray source and a hemispherical PHOIBOS 150 analyzer operating in the fixed analyzer transmission (FAT) mode. The spectra were obtained with a monochromated Al Kα X-ray source (300 W and 14 kV) with a pass-energy of 30 eV. The working pressure in the analyzing chamber was less than 5×10^{-10} kPa. The spectral Pd 3d, Pd 3p, Ag 3d, O 1s, C 1s, Si 2p, Na 1s, Fe 2p, Cr 2p and Al 2p were recorded for each sample. The data treatment was performed with the Casa XPS program (Casa Software Ltd, UK). The peak areas were determined by integration employing a Shirley-type background. Peaks were considered to be a mixture of Gaussian and Lorentzian functions in a 70/30 ratio. For the quantification of the elements, sensitivity factors provided by the manufacturer were used. The depth of analysis of XPS experiments was between 5 and 10 nm.

The XPS analyses were performed on the PdAg composite tubular membranes after being exposed to the dry reforming of methane or hydrogen permeation measurements. After that, the tubular membranes were exposed to ambient conditions, then they were cut in small pieces to be introduced in the ultra high vacuum (UHV) chamber. These membrane pieces were heated up in flowing H_2(5%)/Ar mixture at 400 °C in the reaction chamber of the spectrometer. Later, they were transferred to the XPS spectrometer and the surface characterization was performed.

The PdAg model samples were also analyzed by XPS. Before their introduction into the main chamber of the XPS spectrometer, both samples were annealed at 500 °C in hydrogen flow during 120 h to allow the formation of homogenous PdAg alloys. The XPS spectra were taken on the samples after being exposed to ambient conditions (without in-situ treatment) and after heating in H_2/Ar mixture during 10 min at 400 °C in the pre-treatment chamber attached to the spectrometer.

The effect of the in-situ UHV heat on the surface atomic composition was subsequently studied. The samples, introduced into the main chamber of the spectrometer, were heated up to the desired temperature during 10 min and cooled down to RT; then the XPS spectra were taken. After this measurement, the samples were heated up again to another temperature and subjected to the same procedure described above. The UHV-annealing temperature was increased from 150 to 550 °C.

2.3.2. Angle resolved X-ray photoelectron spectroscopy (ARXPS)

By varying the take-off angle between the direction of the escaping photoelectron and the surface plane of the sample, it was possible to obtain a surface segregation trend in the near-surface region of the reference samples. The measurements under different angles were carried out by tilting the sample with respect to the analyzer. For each ARXPS experiment, measurements were performed at six different angles up to 60° to the surface normal on the model samples after UHV annealing at 500 °C. All spectra were taken in medium area mode, with a spot area about 3 mm. The peaks of the Pd $3d_{5/2}$ and Ag $3d_{5/2}$ were employed for the quantitative analyses.

2.3.3. Elemental depth profiles

XPS depth profiles were acquired on a ThermoFisher Theta Probe instrument, with a base working pressure of $\sim 1.0 \times 10^{-10}$ kPa. A monochromated Al Kα X-ray source and a 50 eV analyzer pass energy were used for the analyses. These analyses were performed on the used PdAg composite membranes after being exposed to ambient conditions and without in-situ treatment in the load-lock chamber of the spectrometer. For each sample, spectra were recorded for Pd 3d, Pd 3p, Ag 3d, Ag 3p, O 1s, C 1s, Fe 2p and Cr 2p photoelectrons. Elemental concentrations were calculated from peak areas, using sensitivity factors and software provided by the instrument manufacturer. Elemental depth profiles were performed using argon ion sputtering. The differentially-pumped ion gun was operated at 1×10^{-8} kPa and 3 kV, conditions which delivered a sputtering rate of approximately 5–10 nm min^{-1}. The sputtering was performed in 5 steps of 10 s, followed by 20 steps of 60 s and 1 step of 600 s to examine the top ~100–200 nm of the membrane surfaces.

3. Results and discussion

To further analyze and compare the surface segregation behavior of several real PdAg membranes, a deeper study was carried out on PdAg model samples synthesized by sequential electroless deposition. Surface alloy formation, atomic composition and segregation at different UHV-annealing temperatures were studied using these samples.

3.1. PdAg reference samples

3.1.1. Surface alloy formation and atomic composition

In order to study the surface properties of electroless plated membranes, two references samples of about 10 μm thick were synthesized on top of Al_2O_3 modified porous stainless steel disks, one of them with a composition similar to the real membranes (PdAg25), and the second one with a lower silver concentration (PdAg10). The low concentration was selected taking into account that the optimal silver atomic composition employed in Pd ternary alloys is close to 10% [17,18]. Before their introduction into the main chamber of the XPS spectrometer, both samples were annealed at 500 °C in hydrogen flow during 120 h to allow the formation of homogenous PdAg alloys. The bulk alloy formation was corroborated by XRD analysis and EDS measurements of the film thickness. The bulk atomic Ag composition measured by EDS was 29 and 10%, respectively.

The annealed PdAg25 reference sample was analyzed by XPS after being exposed to ambient conditions (without in-situ treatment) and after heating in H_2/Ar mixture during 10 min at 400 °C in the pre-treatment chamber attached to the spectrometer. The XPS surface atomic composition of Ag before and after in-situ treatment was about 44% and 42%, respectively. These values were higher than the bulk composition determined by EDS (about 29% Ag). Under annealing up to 500 °C in hydrogen, silver surface segregation took place, which could be due to the lower surface tension of silver with respect to palladium (1.2 and 1.7 J m^{-2} for Ag and Pd, respectively).

On the other hand, it is important to note that the surface concentration of Pd on the in-situ hydrogen-treated sample is slightly higher than the value obtained for the sample exposed to ambient conditions, probably due to the palladium segregation to the surface induced by the higher interaction of Pd with hydrogen. In the same way, Shu et al. [6], through XPS surface characterization of PdAg self-supported membranes, concluded that the chemisorption of H_2 induces palladium segregation.

The possibility of the reversed surface segregation of PdAg alloys in the presence of adsorbed hydrogen has also been reported by Opalka and co-workers from density-functional band-structure investigations [3]. This phenomenon is presumably a consequence of the stronger interaction of hydrogen with Pd. This observation is in agreement with the data reported by Lukaszewski et al. [19]. From Auger electron spectroscopy data, they observed that hydrogen electrosorption on PdAg electrodes significantly affected the surface segregation process [19]. The results revealed that the surface concentration of Pd on the hydrogen-treated samples was significantly higher than before the hydrogen treatment, ranging from 50 to 80%.

Fig. 1A shows the Ag surface composition as a function of the bulk composition for both model samples with different silver concentrations (about 10 and 29%) after being in-situ exposed to H_2. As it can be observed, silver surface segregation with respect to the bulk composition took place in both cases. For comparison purposes, experimental data reported by other groups were added to Fig. 1A. From Auger spectroscopy, Kuijers and Ponce [20] observed a silver surface enrichment for samples prepared by evaporation. It is important to note that the data obtained from the samples studied in the present work are in complete agreement with those reported by Kuijers and Ponec [20].

To complement this study of the surface properties of PdAg samples synthesized by electroless deposition, we also investigated the electronic structure as a function of silver concentration. A pure electroless deposited silver sample was measured as reference resulting in a Ag $3d_{5/2}$ binding energy of 368.3 eV, in agreement with data previously reported for Ag foils [21]. A shift toward a lower binding energy of the Ag $3d_{5/2}$ peak (367.5–367.7 eV) was observed in both samples after annealing when compared to the metallic silver (368.3 eV), suggesting the alloy formation on the surface. On the other hand, the binding energy for the Pd $3d_{5/2}$ feature did not present a significant shift with respect to that of metallic Pd (BE = 335.1 ± 0.1 eV). Fig. 1B shows the Ag $3d_{5/2}$ binding energy as a function of [Ag/(Pd + Ag)] for the PdAg25, PdAg10 and pure Ag reference samples (close symbols). Data from the PdAg real membranes were included for comparison (open symbols). From this figure, it is clear that as the Ag concentration is increased there is a monotonous shift toward the higher binding energy of the Ag $3d_{5/2}$ core-level peak. Chae et al. [22] reported a study of electronic structure in ion-beam-mixed PdAg alloys and found that the Ag $3d_{5/2}$ core-level generally shifts to a lower binding energy for samples with higher palladium composition. The redistribution of the valence electrons associated with the change of the chemical bond leads to a change of energies of the core levels of atoms participating in the bond. Similarly, for thick co-evaporated PdAg-alloy films, Steiner and Hüfner [23] reported an almost linear shift of the Ag 3d peak position with increasing Pd concentration.

3.1.2. *Effect of the UHV-annealing temperature on the surface composition*

After the previous experiments, the effect of the UHV-annealing temperature on the surface composition of the PdAg electroless plated samples was investigated using XPS. Fig. 2 shows the XPS data taken from the PdAg25 reference sample as a function of the UHV-annealing temperature for two different emission angles. It can be observed that the relative surface concentration of the metals as a function of temperature shows three different regions. At low temperature (between 150 and 300 °C), the metal surface concentration remained practically constant, with a Pd and Ag surface

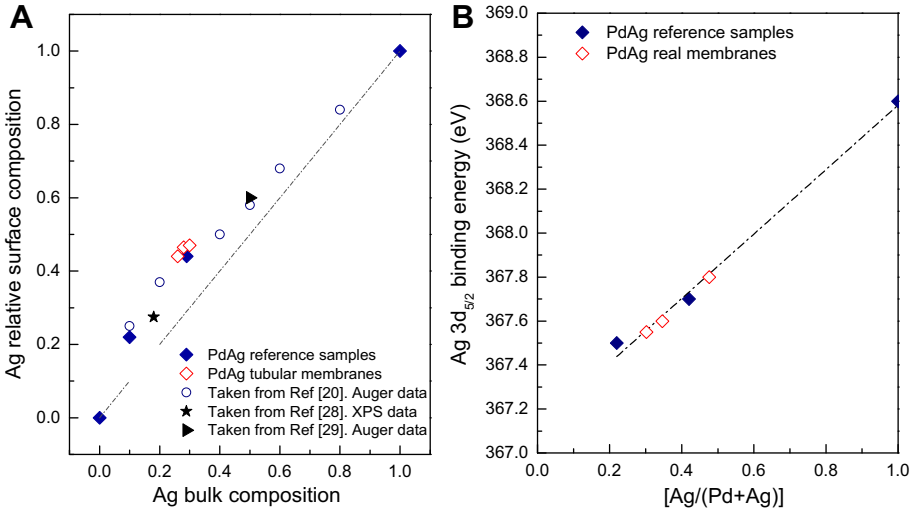

Fig. 1 – (A) Surface vs. bulk silver composition; (B) Ag $3d_{5/2}$ binding energy as a function of [Ag/(Pd + Ag)] for different samples. PdAg reference samples: data taken after exposure to hydrogen in the reaction chamber. PdAg real membranes (PdAg-40-500/Al_2O_3, PdAg-40-550/Al_2O_3 and PdAg-40-550/NaA-HS): without treatment in the spectrometer.

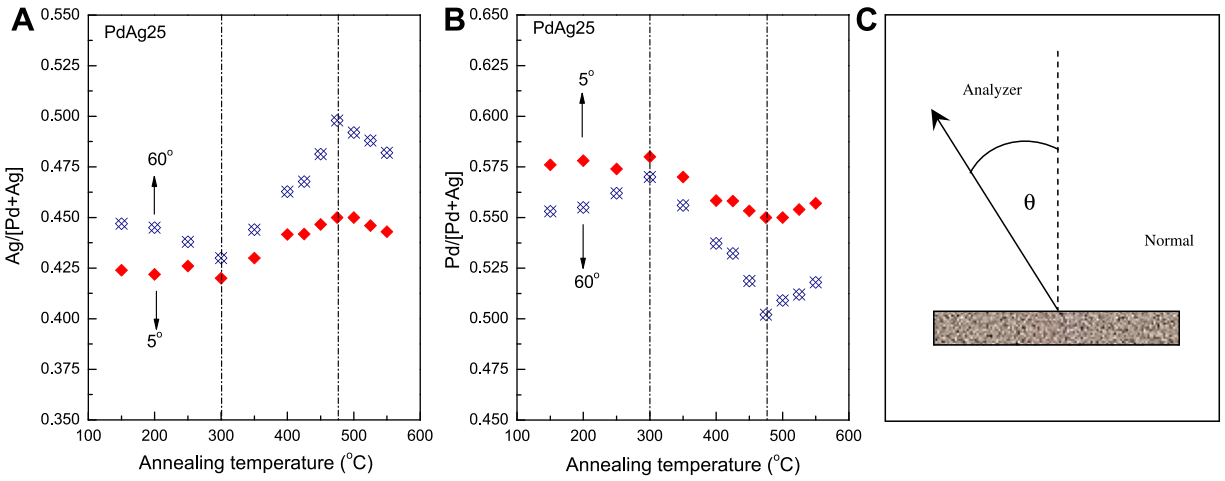

Fig. 2 – Ag (A) and Pd (B) atomic surface composition as a function of the in-situ annealing temperature for the PdAg25 reference sample. (C) Scheme of the ARXPS measurement.

concentration of about 57% and 43% at the lower emission angle, respectively. From 300 °C, the silver percentage on the surface increased with temperature up to about 475 °C. At higher temperatures, the Ag concentration decreased with increasing temperature. It should be noted that for both emission angles the trend is similar, being more pronounced in the most surface region (higher emission angle) (Fig. 2). For the PdAg10 alloy, the same behavior was observed when the UHV-annealing temperature was increased (Fig. 3).

The behavior observed as a function of temperature could be explained by the adsorption of H_2 during the thermal treatment in the load-lock chamber of the spectrometer. As expressed above, due to a higher interaction between Pd and H_2, palladium surface segregation is predicted to occur [3]. At about 300 °C [24], hydrogen started to desorb from the surface, and silver atomic composition on the surface increased up to about 475 °C. At higher temperatures, where the alloy reached equilibrium (between the bulk and surface composition), it was possible to observe a behavior similar to the one predicted by the McLean equation (Figs. 2 and 3). For a PdCu alloy, Miller et al. [25] found a similar effect in the surface composition as a function of temperature through ISS and XPS measurements. At about 520 °C, the PdCu alloy reached the equilibrium state, then at higher temperatures, the XPS surface composition followed the tendency predicted by the McLean equation.

In order to further support the above explanation, the desorption of hydrogen at about 275–300 °C was followed by the use of a mass spectrometer. The PdAg10 reference sample was reduced in H_2 5%/Ar at 400 °C during 10 min, and then introduced into the main chamber of the spectrometer. After that, the heating procedure was repeated at 150 and 300 °C with the mass spectrometer turned on. From these experiments, an increase in the base pressure of the spectrometer and a desorption peak assigned to H_2 were observed, which was in agreement with the surface segregation behavior of the samples as a function of temperature.

The near-surface region depth profile for the PdAg25 sample was obtained using ARXPS after UHV annealing up to

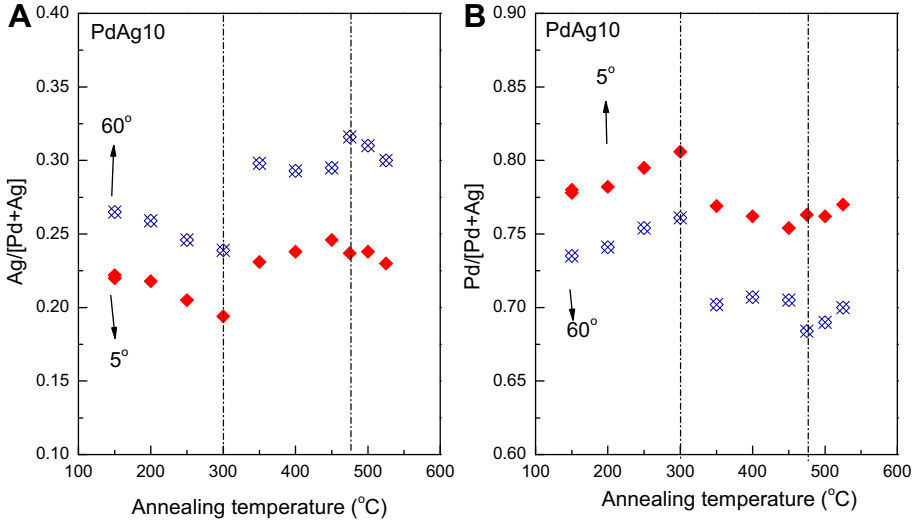

Fig. 3 – Ag (A) and Pd (B) atomic surface composition as a function of the in-situ annealing temperature for the PdAg10 reference sample.

500 °C in the main chamber of the spectrometer (Fig. 4). It is possible to note that the silver concentration increased with the emission angle (more surface sensitive), showing that silver segregation took place in the near-surface region.

The behavior of the valence-band spectra for the reference sample is shown in detail in Fig. 5. The spectrum of the sample clearly shows two well-resolved bands at about 5.5 and 2.8 eV assigned to Ag, and Pd, respectively. Close to the Fermi level, we can observe the Pd 4d bands, which extend over a region of about 5 eV below the Fermi level as reported in the literature [26]. On the other hand, the pure silver spectrum has two features at about 4.5 and 6.5 eV, corresponding to the Ag sp band and d state band, respectively [7]. The valence-band spectra of sample PdAg25 as a function of the emission angle shows a slow increase in the Ag contribution (about 6–8 eV) as the emission angle increases (Fig. 5). These results are in agreement with the ARXPS data of the core levels (Fig. 4).

3.2. *Performance and surface states of real PdAg composite membranes*

Surface segregation behavior and alloy formation of several real PdAg composite membranes were investigated after high temperature hydrogen permeation and reaction measurements. The membranes were synthesized by electroless deposition technique on the outer surface of porous stainless steel tubes using a metallic short deposition time (40 min) in order to obtain a homogeneous bulk composition. Similar membranes were previously synthesized and evaluated at high temperature. In these samples, the Knudsen and viscous contributions to the total hydrogen flux were quantified [13].

To evaluate the performance of the membranes presented in this work, hydrogen permeation measurements were

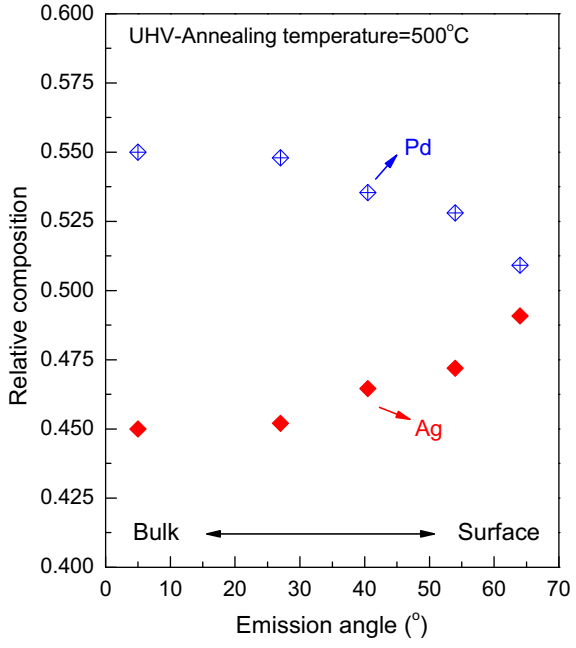

Fig. 4 – Pd and Ag surface composition as a function of the emission angle for the PdAg25 sample after annealing at 500 °C.

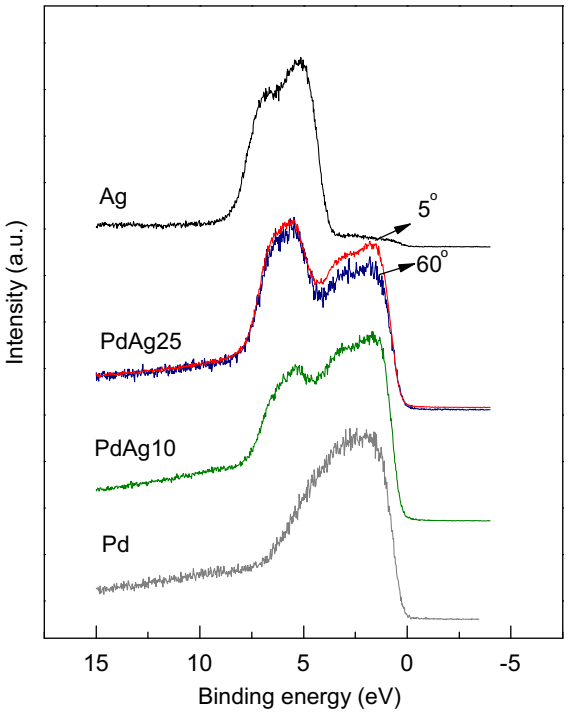

Fig. 5 – Valence-band spectrum of the reference samples compared with those of Pd and Ag.

carried out at 400, 425 and 450 °C as a function of transmembrane pressure. A linear increase of the H_2 permeation flow with the difference of the square root of the hydrogen partial pressure was observed for all composite membranes (data not shown). This behavior suggests that the diffusion of hydrogen in the metallic film mainly obeys Sieverts' law. For these membranes, the hydrogen permeance and H_2/N_2 ideal selectivity (defined as the ratio between the flux rates of H_2 and N_2) are given in Table 1. In order to study the performance of the samples under reaction conditions, the membranes PdAg-40-500/Al_2O_3 and PdAg-40-550/NaA-HS were used in a membrane reactor for the dry reforming of methane at 450 °C, using a Rh/La_2O_3 catalyst. In both cases, the value of CH_4 conversion at 450 °C (between 12 and 15%) were higher than those obtained in the fixed-bed reactor, with a hydrogen recovery between 65 and 79%.

The XRD and EDS data suggest that a PdAg homogeneous alloy was formed throughout the whole thickness of the membranes. From the EDS data a volumetric silver composition ca. 25% was observed in the three samples. Neither the crystalline structure nor the morphology of the membranes were affected by the permeation and reaction conditions.

From the XPS data, a shift toward a lower binding energy of the Ag $3d_{5/2}$ peak (367.6–367.8 eV) was observed in the membrane when compared to the pure metallic silver (368.3 eV), suggesting the alloy formation on the surface. On the other hand, the binding energy for the Pd $3d_{5/2}$ feature did not present a significant shift with respect to that of metallic Pd (BE = 335.1 ± 0.1 eV). The Ag surface concentration (XPS) was considerably higher than the volumetric one determined by EDS (Table 1, Fig. 1A). In agreement with the results

Table 1 – Main properties of the PdAg real membranes.

Membrane	Permeance × 10^4 (mol m^{-2} $s^{-1}Pa^{-0.5}$)	Ideal selectivity (H_2/N_2)	Treatment	Ag XPS[d]	Ag EDS surface[e]
PdAg-40-550/Al_2O_3	9.1	110[a]	Permeation	47.4	30
PdAg-40-550/NaA-HS	21	215[b]	Permeation-reaction[c]	46.5	28
PdAg-40-500/Al_2O_3	5.6	170[a]	Permeation-reaction[c]	44.0	26

a Data obtained at 100 kPa.
b Data obtained at 40 kPa.
c Time on reaction = 52 h.
d Measured in the Spect instrument, after reduction in H_2 (5%)/Ar during 10 min.
e Value measured in a top view of the membrane with a magnification of 60×.

obtained from the reference samples, this behavior can be related to the low Ag surface tension with respect to Pd. In Fig. 1A, the silver surface composition as a function of the bulk composition is presented for the membranes PdAg-40-500/Al_2O_3, PdAg-40-550/Al_2O_3 and PdAg-40-550/NaA-HS. Note that the extension of the silver surface segregation on the real membranes was in agreement with the data reported for the PdAg25 model samples.

3.3. *XPS depth profile analysis of real PdAg membranes*

In order to analyze the surface segregation effects under reaction conditions and after permeation experiments, the PdAg-40-500/Al_2O_3, PdAg-40-550/Al_2O_3 and PdAg-40-550/NaA-HS membranes, which showed a homogeneous cross section concentration from EDS, were analyzed by XPS as a function of Ar^+ sputtering time. XPS wide scan spectra revealed that the impurities of carbon and oxygen were present besides palladium and silver. Carbon contamination concentration at the top surface of the membranes decreased with sputtering time and was no longer detectable after 60 s. No signal for either Fe or Cr was detected. The Ag and Pd relative surface composition as a function of the sputtering time is shown in Fig. 6. After about 50 s of sputtering, the three samples reached a homogeneous composition (about 30%), showing silver enrichment with respect to the bulk composition determined by EDS in the three samples (Table 1). It is important to note that no significant difference was observed with Ar^+ sputtering time for the PdAg-40-550/Al_2O_3 sample, which was analyzed after permeation experiments and the other samples which were measured after being used in the membrane reactor for the dry reforming of methane reaction. For PdAg membranes synthesized by deposition cycles of 90 min and annealing at different temperatures, a similar Ag segregation was reported reaching a homogeneous composition at about 60 s of sputtering [8]. This behavior of the surface composition as a function of the sputtering time was similar for the samples evaluated in reaction and after hydrogen permeation experiments. These data are in agreement with the ARXPS results of the PdAg25 reference sample where silver surface segregation was observed in the near-surface region.

During the depth profile experiments, the evolution of the Pd and Ag surface species was also analyzed. Fig. 7 shows the Pd 3d spectra of the PdAg-40-500/Al_2O_3, PdAg-40-550/Al_2O_3 and PdAg-40-550/NaA-HS membranes at several Ar^+ sputtering time. It can be observed that the features of the three samples before sputtering could be fit as the contribution of two components, one peak located at about 335.7 eV and a second peak at 335.1 eV. The high binding energy contribution of the Pd $3d_{5/2}$ signal could be originated from the PdO_x ($0 < x < 1$) formation at the surface level, and the lower binding energy peak could be due to the Pd metallic contribution. From the curve fitting of the Pd 3p–O 1s region (not shown) it was

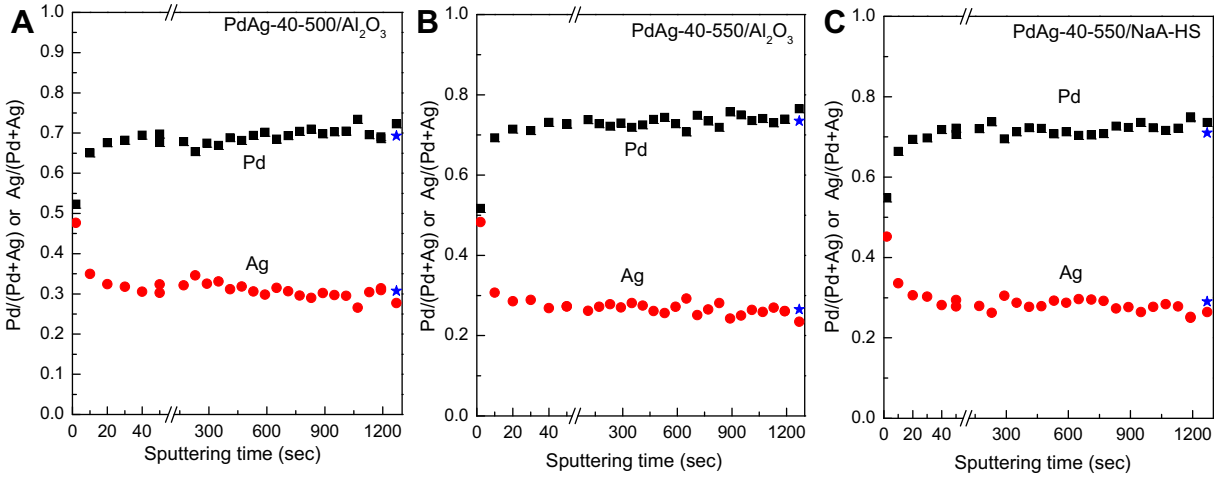

Fig. 6 – XPS [Ag/(Pd + Ag)] and [Pd/(Pd + Ag)] ratio as a function of the sputtering time for the PdAg-40-500/Al_2O_3 (A), PdAg-40-550/Al_2O_3 (B) and PdAg-40-550/NaA-HS (C) membranes. ★: Data taken after 1790 s of sputtering.

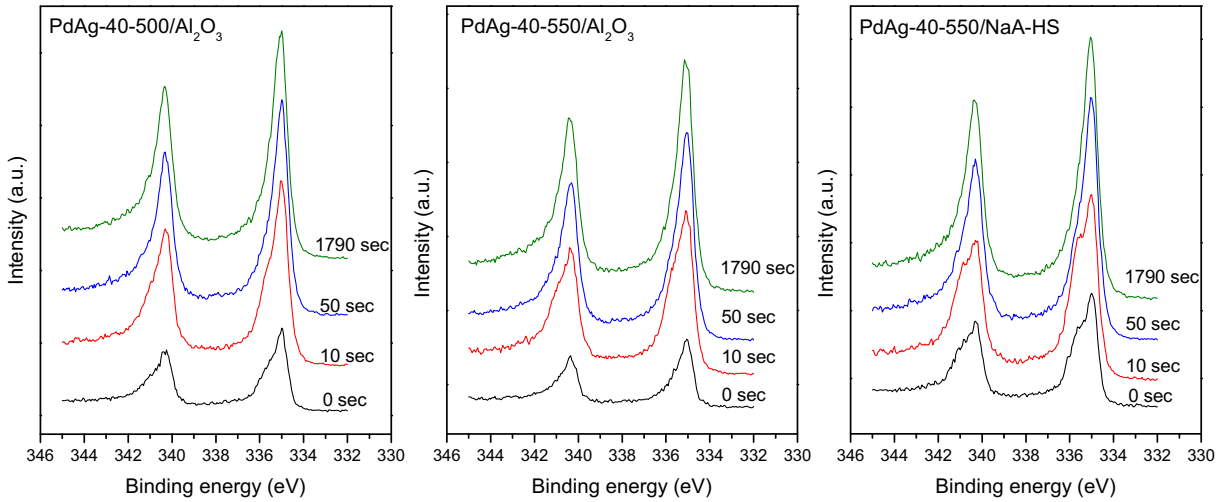

Fig. 7 – Pd $3d_{5/2}$ core-level spectra at different sputtering times for the membranes: PdAg-40-500/Al_2O_3, PdAg-40-550/Al_2O_3 and PdAg-40-550/NaA-HS.

possible to determine that the three samples contained a similar proportion of oxygen on the surface (10–15%) which was no longer detectable after 50 s of Ar^+ sputtering, indicating that PdO_x or PdO was present only on the top surface.

In agreement with the interpretation presented by Bosko et al. [8], the Pd $3d_{5/2}$ higher binding energy peak could be assigned to the formation of PdO_x species after air exposure of the membranes before the introduction into the XPS-chamber. For sputtered as-grown PdAg films, Ramachandran et al. [27] observed a binding energy chemical shift of about 0.61 ± 0.3 eV to higher binding energy relative to the bulk Pd contribution, due to exposure of the sample to air before introduction into the spectrometer. In the same way, Yang et al. [28], using XPS, reported that the presence of a higher binding energy peak at 335.5 eV indicated a new structure PdO_x ($0 < x < 1$) in a PdAg membrane.

Fig. 8 shows the evolution of the Pd $3d_{5/2}$ and Ag $3d_{5/2}$ core-level peaks with sputtering time for the PdAg-40-500/Al_2O_3 membrane. The vertical lines indicated the binding energy position of the Pd $3d_{5/2}$ and the Ag $3d_{5/2}$ metallic component. As seen from the spectra, the Ag $3d_{5/2}$ peak showed a slight shift to lower binding energy after sputtering time, which could be related to a partial oxidation of silver during the transfer of the sample to the spectrometer, in the same way as Pd showed a second peak with high binding energy. However, Yang et al. [28] studied the effect of thermal treatment at 400 °C in air of a PdAg sample prepared by electroless plating and reported the formation of PdO_x species, while the Ag $3d_{5/2}$ core-level peak remained unchanged. From that observation, it is possible to conclude that for the PdAg membranes studied in this work, the Ag $3d_{5/2}$ shift could not be due to oxidation. This change could be related to the decrease in Ag surface composition with sputtering time, as shown from the depth profile experiments (Fig. 6).

In Fig. 8C, the binding energy shift of the Pd $3d_{5/2}$ and Ag $3d_{5/2}$ peaks is shown as a function of the Pd atomic surface

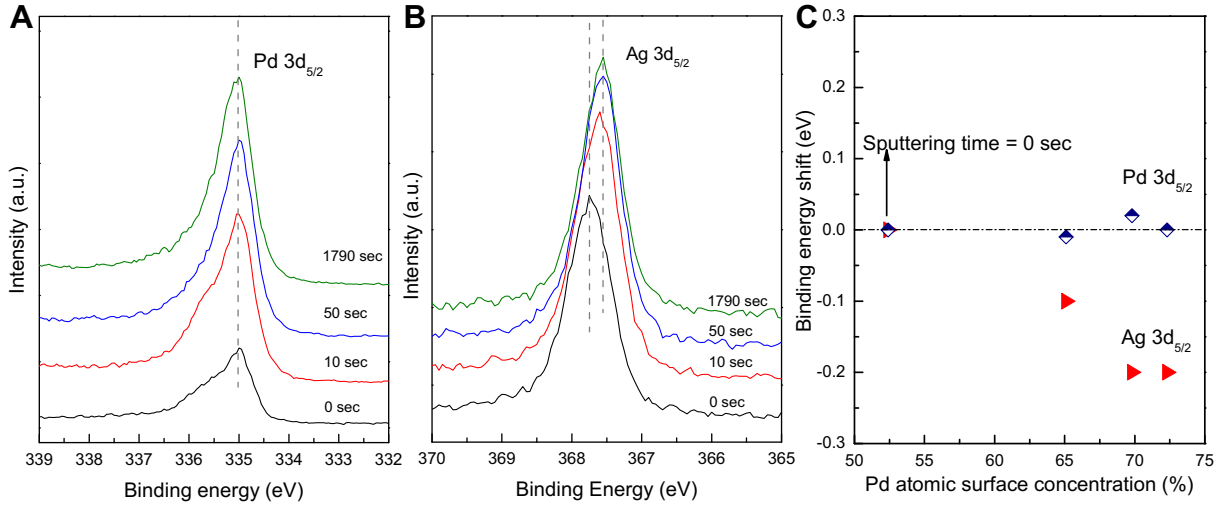

Fig. 8 – (A) Pd $3d_{5/2}$ and (B) Ag $3d_{5/2}$ core-level spectra at different Ar^+ sputtering times. (C) Pd $3d_{5/2}$ and Ag $3d_{5/2}$ shift at a function of Pd atomic surface concentration for PdAg-40-500/Al_2O_3.

composition for the PdAg-40-500/Al_2O_3 membrane during sputtering experiments. It is important to note that the Pd $3d_{5/2}$ peak assigned to the metallic contribution remained practically constant, while the Ag $3d_{5/2}$ shifted up to about −0.2 eV. Note that this shift toward lower binding energy observed in the Ag $3d_{5/2}$ peak with the Ar^+ sputtering time (decrease in Ag surface composition), is in complete agreement with the tendency observed with the reference samples (Fig. 1B).

4. Conclusions

Silver surface enrichment of electroless plated films after annealing up to 500 °C in hydrogen was corroborated by means of XPS and ARXPS experiments. A relationship between the Ag $3d_{5/2}$ core-level binding energy shift and the silver surface composition was observed from the XPS data obtained with the model samples.

Increasing the in-situ annealing temperature results in an increase of the Ag surface composition from 300 to 475 °C. At greater temperatures, where the equilibrium alloy was reached, a decrease in the Ag composition was observed in agreement with the tendency predicted by the McLean equation.

The XPS depth profile analysis of the real PdAg composite membranes indicated that after both hydrogen permeation and reaction experiments, silver surface segregation took place, showing the same behavior as the model samples.

A good agreement between the Ag atomic surface compositions of our electroless plated samples and those reported in the literature using other synthesis methods was observed. This fact shows that the synthesis method used to prepare PdAg-alloy membranes has no significant effect on the surface segregation tendency.

Acknowledgments

The authors wish to acknowledge the financial support received from UNL, CONICET and ANPCyT. They are also grateful to the Japan International Cooperation Agency (JICA) for the donation of the XRD and to ANPCyT for Grant PME 8-2003 to finance the purchase of the UHV Multi Analysis System. Thanks are given to Prof. Elsa Grimaldi for the English language editing. Finally, the authors wish to express their thanks to Prof. Andrew Gellman and James Miller for being able to carry out the depth profile measurements in their lab.

REFERENCES

[1] Ropo M, Kokko K. Segregation at the PdAg(111) surface: electronic structure calculations. Phys Rev B 2005;71: 0454111–6.
[2] Ma Y, Bansmann J, Diemant T, Behm RJ. Formation, stability and CO adsorption properties of PdAg/Pd(111) surface alloy. Surf Sci 2009;603:1046–54.
[3] Lovvik OM, Opalka SM. Reversed surface segregation in palladium–silver alloys due to hydrogen adsorption. Surf Sci 2008;602:2840–4.
[4] Chen FL, Sakamoto KF, Nakayama Y, Sakamoto Y. Hydrogen permeation through palladium-based alloy membranes in mixtures of 10% methane and ethylene in the hydrogen. Int J Hydrogen Energy 1996;210:555–61.
[5] Sakamoto Y, Chen FL, Kinari Y, Sakamoto F. Effect of carbon monoxide on hydrogen permeation in some palladium-bases alloy membranes. Int J Hydrogen Energy 1996;210:1017–24.
[6] Shu J, Adnot A, Grandjean BPA, Kaliaguine S. Structurally stable composite Pd–Ag alloy membranes: introduction of a diffusion barrier. Thin Solid Films 1996;286:72–9.
[7] Peters TA, Tucho WM, Ramachandran A, Stange M, Walmsley JC, Holmestad R, et al. Thin Pd–23%Ag/stainless steel composite membranes: long-term stability, life-time estimation and post-process characterization. J Membr Sci 2009;326:572–81.
[8] Bosko ML, Miller JB, Lombardo EA, Gellman AJ, Cornaglia LM. Surface characterization of Pd–Ag composite membranes after annealing at various temperatures. J Membr Sci 2011; 369:267–76.
[9] Gade SK, Keeling MK, Davidson AP, Hatlevik O, Way JD. Palladium–ruthenium membrane for hydrogen separation fabricated by electroless co-deposition. Int J Hydrogen Energy 2009;34:6486–91.
[10] Shi L, Goldbach A, Zeng G, Xu H. Preparation and performance of thin-layered PdAu/ceramic composite membrane. Int J Hydrogen Energy 2010;35:4201–8.
[11] Chi Y-H, Yen P-S, Jeng M-S, Ko S-T, Lee T-C. Preparation of thin Pd membrane on porous stainless steel tubes modified by a two-step method. Int J Hydrogen Energy 2010;35: 6303–10.
[12] Ryi S-K, Xu N, Li A, Lim CJ, Grace JR. Electroless Pd membrane deposition on alumina modified porous Hastelloy substrate with EDTA-free bath. Int J Hydrogen Energy 2010;35:2328–35.
[13] Bosko ML, Lombardo EA, Cornaglia LM. The effect of electroless plating time on the morphology, alloy formation and H_2 transport properties of Pd–Ag composite membranes. Int J Hydrogen Energy 2011;36:4068–78.
[14] Guazzone F, Engwall EE, Ma YH. Effects of surface activity, defects and mass transfer on hydrogen permeance and *n*-value in composite palladium-porous stainless steel membranes. Catal Today 2006;118:24–31.
[15] Mardilovich PP, She Y, Ma YH, Rei M. Defect-free palladium membranes on porous stainless-steel support. AIChE J 1998; 44:310–22.
[16] Bosko ML, Múnera JF, Lombardo EA, Cornaglia LM. Dry reforming of methane in membrane reactors using Pd and Pd–Ag composite membranes on a NaA zeolite modified porous stainless steel support. J Membr Sci 2010;364:17–26.
[17] Ling C, Semidey-Flecha L, Sholl DS. First-principles screening of PdCuAg ternary alloys as H_2 purification membranes. J Membr Sci 2011;375:189–96.
[18] Tarditi AM, Braun F, Cornaglia LM. Novel PdAgCu ternary alloy: hydrogen permeation and surface properties. Appl Surf Sci 2011;257:6626–35.
[19] Lukaszewski M, Klimerk K, Czerwinski A. Microscopic, spectroscopic and electrochemical characterization of the surface of Pd–Ag alloys. J Electroanal Chem 2009;637:13–20.
[20] Kuijers FJ, Poned V. The surface composition of Pd–Ag alloys. J Catal 1979;60:100–9.
[21] Waterhouse GIN, Bowmaker GA, Metson JB. Oxidation of polycrystalline silver foil by reaction with ozone. Appl Surf Sci 2001;183:191–204.
[22] Chae KH, Lee YS, Whang CN, Leon Y, Choi BS, Croft M. Charge redistribution in ion-beam-mixed Pd–Ag alloys. Nucl Instr. Meth B 1996;117:123–8.
[23] Steiner P, Hüfner S. Thermochemical analysis of Pd_xAg_{1-x} alloy from XPS core-level binding energy shifts. Solid State Commun 1981;37:79–81.

[24] Noordermeer A, Kok GA, Nieuwenhuys BE. A comparative study of the behavior of the PdAg(111) and Pd(111) surfaces towards the interaction with hydrogen and carbon monoxide. Surf Sci 1986;165:375–92.
[25] Miller JB, Matranga CH, Gellman AJ. Surface segregation in a polycrystalline $Pd_{70}Cu_{30}$ alloy hydrogen purification membrane. Surf Sci 2008;602:375–82.
[26] Tarditi AM, Cornaglia Laura M. Novel PdAgCu ternary alloy as promising materials for hydrogen separation membranes: synthesis and characterization. Surf Sci 2011;605:62–71.
[27] Ramachandran A, Tucho WM, Mejdell AL, Stange M, Venvik HJ, Walmsley JC, et al. Surface characterization of Pd/Ag 23 wt% membranes after different thermal treatments. Appl Surf Sci 2010;256:6121–32.
[28] Yang L, Zhang Zh, Gao X, Guo Y, Wang B, Sakai O, et al. Changes in hydrogen permeability and surface state of Pd–Ag/ceramic composite membranes after thermal treatment. J Membr Sci 2005;252:145–54.
[29] Wouda PT, Schmid M, Nieuwenhuys BE, Varga P. STM study of the (111) and (100) surface of PdAg. Surf Sci 1998;417:292–300.